Available online at www.sciencedirect.com
SCIENCE DIRECT®
Journal of Solid State Chemistry 172 (2003) 277–287
JOURNAL OF SOLID STATE CHEMISTRY
http://elsevier.com/locate/jssc

The systems Zr(Nb,Ti)(R)$O_{2-\delta}$, R = Yb, Ca—optimization of mixed conductivity and comparison with results of other systems (R = Y and Gd)

D.P. Fagg,[a,*] A.J. Feighery,[b] and J.T.S. Irvine[b]

[a] *Department of Ceramics and Glass Engineering, CICECO, University of Aveiro, Aveiro 3810-193, Portugal*
[b] *StACAM University of St. Andrews Purdie Building, St. Andrews, Fife, Scotland KY16 9ST, UK*

Received 11 October 2002; received in revised form 3 January 2003; accepted 8 January 2003

Abstract

In this work we address the optimization of mixed conductivity in fluorite compounds based on zirconia. Phase relations of the new systems $YbO_{1.5}$–$NbO_{2.5}$–ZrO_2, and CaO–$NbO_{2.5}$–ZrO_2 are presented. The limit of the cubic defect fluorite phase in $YbO_{1.5}$–$NbO_{2.5}$–ZrO_2 closely resembles that of the system $YO_{1.5}$–$NbO_{2.5}$–ZrO_2, whilst in CaO–$NbO_{2.5}$–ZrO_2 is narrow extending to include composition $Ca_{0.255}Nb_{0.15}Zr_{0.595}O_{1.82}$ at 1500°C. The influence of dopant ion size, charge and composition on ionic conduction is assessed and parallels are drawn with the systems $YO_{1.5}$–$NbO_{2.5}$–ZrO_2 and $YO_{1.5}$–TiO_2–ZrO_2. Comparison of these results with published data on the Ti containing systems CaO–TiO_2–ZrO_2, $GdO_{1.5}$–TiO_2–ZrO_2 shows that the highest mixed conducting compositions can only be offered in the system $YO_{1.5}$–TiO_2–ZrO_2 out of all the systems here studied.

Keywords: Fluorite; Mixed conductor; Zirconia; Oxygen ionic conductor; Phase relations

1. Introduction

Many fluorite-based oxides offer good oxide-ion conductivity and it is possible to dope these existing high, ionically conducting materials with small concentrations of variable valence ions, such as the early transition metals Ti and Nb, to produce a significant electronic contribution to the total conductivity when in reducing atmospheres. Previous work has shown that the electronic contribution to mixed conduction increases with the concentration of these transition metal ions [1–3]. Unfortunately, at the levels of doping required to achieve a reasonable electronic enhancement, the magnitude of the ionic component is often impaired [3,4].

The system $YO_{1.5}$–$NbO_{2.5}$–ZrO_2 exhibits a large defect fluorite solid solution and was previously adopted as a base model with which to assess this suppression of ionic conductivity, with a view to facilitating prediction of the composition dependence of conductivity in other similar fluorite zirconia-based mixed conducting systems [5–12]. A thorough ionic conductivity study was performed across the defect fluorite solid solution and indicated that the activation energy for conduction increases rapidly whilst isothermal conductivity decreases as yttria content increases. These observations have recently been confirmed in work by other authors [13,14]. At high defect concentrations (>30–35 at% Y) activation energies tend to a constant value of around 1.3 eV. Although phase analysis by X-ray powder diffraction clearly indicates extensive ranges of cubic fluorite solid solution, both neutron and electron diffraction techniques revealed that on the atomic or nano-scales there is a high degree of inhomogeneity [10,11]. The decrease in isothermal conductivity correlated with increasing intensity of diffuse features in neutron diffraction experiments and with increases in the isotropic temperature factor of the anion sublattice, features which are evidence of domain formation. An inverse relationship was observed between conductivity pre-factor and oxygen temperature factors [10,11]. Electron diffraction studies showed that these diffuse reflections can be considered to be a mixture of C-type

*Corresponding author. Fax: +351-234-425300.
E-mail address: duncan@cv.ua.pt (D.P. Fagg).

0022-4596/03/$ - see front matter © 2003 Elsevier Science (USA). All rights reserved.
doi:10.1016/S0022-4596(03)00086-0

and distorted pyrochlore (P-type structure) [11]. Compositions close in composition to $Zr_{0.5}Y_{0.5}O_{1.75}$ exhibit weak satellite reflections related to atomic ordering which is predominantly C-type cubic in nature whilst those close to $Y_{0.75}Nb_{0.25}O_{1.75}$ exhibit atomic ordering characteristic of the pyrochlore P-type structure.

The apparent defect fluorite solid solution in the system $YO_{1.5}$–$NbO_{2.5}$–ZrO_2, therefore, presents a "short range" atomic ordering which can be considered as a gradual transition between two fluorite related structures; the C-type and the distorted P-type structures, as has been determined in other defect fluorite systems such as CeO_2–$YO_{1.5}$ and ZrO_2–$PrO_{1.5}$ [15,16].

Recently, detailed experimental phase diagrams of the systems $YO_{1.5}$–TiO_2–ZrO_2 [17,18], $GdO_{1.5}$–TiO_2–ZrO_2 [19], and CaO–TiO_2–ZrO_2 [20,21] have been published. Some of these systems exhibit extensive regions of cubic defect fluorite solid solution, supporting theoretically calculated phase diagrams published by Yokokawa et al. [22]. In this study we present ionic conductivity behavior and phase relations for the new systems $YbO_{1.5}$–$NbO_{2.5}$–ZrO_2, CaO–$NbO_{2.5}$–ZrO_2 and combine the results with those of the similar systems $YO_{1.5}$–$NbO_{2.5}$–ZrO_2, CaO–TiO_2–ZrO_2, $GdO_{1.5}$–TiO_2–ZrO_2, and $YO_{1.5}$–TiO_2–ZrO_2. Focus is concentrated on maximizing ionic conduction whilst maintaining significant concentration of variable valent ions in the search for peak mixed conducting compositions.

2. Experimental

Yttria, ytterbia, calcium carbonate, niobia, titania (Aldrich) and zircona (Tioxide) powders of purity 99.99%, were used as the starting materials. To remove moisture and absorbed gases, it was necessary to dry Y_2O_3 and Yb_2O_3 powders for 24 h at 1000°C and to weigh directly from a desiccator. ZrO_2, TiO_2 and Nb_2O_5 powders were dried at 700°C for 24 h. Stoichiometric amounts of these powders were intimately ground under acetone using an agate pestle and mortar and dry pressed into pellets under a pressure of 3 ton/cm^2. All powder weighed was included in the pellet. Samples were fired in air at 1500°C for 32 h followed by fast cooling to room temperature. Phase purity, lattice parameters and thermal expansion data were determined by powder X-ray diffraction using a Stoe Stadi-P diffractometer. For electrical measurements an organo-platinum paste was painted on each face of the pellets and sintered at 1000°C. No structural changes are observed on annealing at this temperature. Bulk Arrhenius conductivity plots were obtained by AC impedance using a Schlumberger Solatron 1260 Frequency Response Analyzer coupled with a 1287 Electrochemical Interface controlled by Zplot electrochemical impedance software. Corrections were made for jig impedance, stray capacitance, and sample density [23]. Sample densities were in the range 75–90% that of the theoretical. Stabilization time at each temperature was 30 min.

3. Results and discussion

3.1. System $YO_{1.5}$–$NbO_{2.5}$–ZrO_2

The phase limits and conductivity of this system have previously been extensively studied [5–14]. The phase diagram is reproduced in Fig. 1 from Ref. [8], showing compositions studied for conductivity [7–11]. Adequate summary of the conductivity behavior of the cubic fluorite phase is to be found in Refs. [8,10]. For any fixed niobium concentration the highest ionic conductivity is found on the low Y_2O_3, high ZrO_2 edge of the solid solution. This corresponds to a join linking the compositions $Y_{0.15}Zr_{0.85}O_{1.93}$ and $Y_{0.75}Nb_{0.25}O_{1.75}$, (join a).

3.2. System $YbO_{1.5}$–$NbO_{2.5}$–ZrO_2

3.2.1. Extent of the cubic defect fluorite phase

Much work has been done on the binary systems $Zr(R)O_{2-y}$ where R = Sm, Y, Yb, Sc or Ca and several reviews and compilations exist [24,25]. The low Yb limit of the defect fluorite solid solution on this join is reported by Gonzalez et al. [26] to be in the region of 6–7 at% Yb. The join $YbO_{1.5}$–$NbO_{2.5}$ has been little studied, but work can be found on the closely related

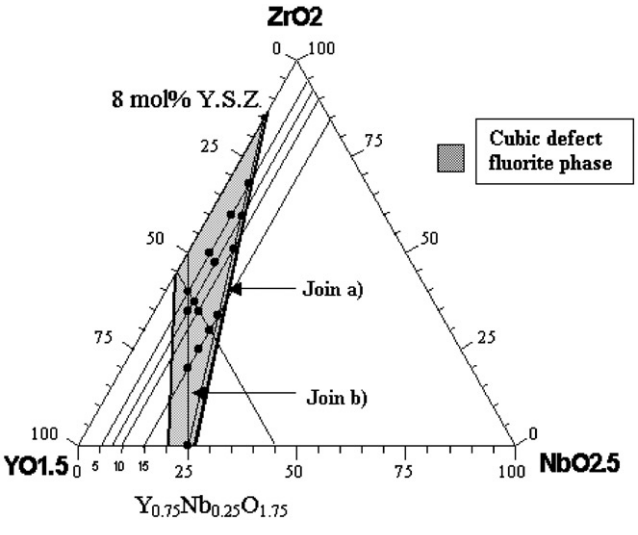

Fig. 1. The limit of the cubic defect fluorite solid solution in the system $YO_{1.5}$–$NbO_{2.5}$–ZrO_2, from Ref. [8]. The shaded region corresponds to the cubic defect fluorite phase, while points indicate compositions studied for conductivity in Refs. [7–11]. Join (a) = $Y_{(0.15+0.6x)}Nb_{0.25x}Zr_{(0.85-0.85x)}O_{(1.93-0.18x)}$, join (b) = $Y_{(0.5+0.25x)}Nb_{0.25x}Zr_{(0.5-0.5x)}O_{1.75}$ ($0 \leqslant x \leqslant 1$).

system $YbO_{1.5}$–$TaO_{2.5}$ [27] showing the presence of the cubic fluorite phase in a narrow compositional range around that of $Yb_{0.75}Ta_{0.25}O_{1.75}$.

The chemical and physical properties of the ions yttrium and ytterbium are very similar, as are the relative ionic radii of Y and Yb in eightfold sites (1.019 and 0.985 Å), respectively [28]. This leads to the expectation that the phase diagrams and conductivity behavior of $YO_{1.5}$–$NbO_{2.5}$–ZrO_2 and $YbO_{1.5}$–$NbO_{2.5}$–ZrO_2 might also be similar.

Compositions along the join $Yb_{(0.15+0.6x)}Nb_{0.25x}Zr_{(0.85-0.85x)}O_{(1.93-0.18x)}$ $(0 \leqslant x \leqslant 1)$ were studied as this join was found to be the low yttria, high zirconia phase edge of the fluorite solid solution in the closely related system $YO_{1.5}$–$NbO_{2.5}$–ZrO_2 and, as such, offered compositions of the highest ionic conductivity for any fixed niobium concentration. In the Yb system all compositions along this join were observed by X-ray diffraction to be solely that of the cubic defect fluorite phase with no impurity peaks present. To assess the extent of the cubic solid solution in the Yb-system, further compositions were analyzed around the intersects of this join with the binary ZrO_2–$YbO_{1.5}$ and $YbO_{1.5}$–$NbO_{2.5}$ joins together with ternary compositions outwith join $Yb_{(0.15+0.6x)}Nb_{0.25x}Zr_{(0.85-0.85x)}O_{(1.93-0.18x)}$ in the direction of increasing niobia, Fig. 2.

The low ytterbia phase limit of the defect fluorite solid solution on the binary join $YbO_{1.5}$–$NbO_{2.5}$ lies between 26 and 27 mol% $NbO_{2.5}$. The corresponding phase limit on the binary join $YbO_{1.5}$–ZrO_2 lies between 11 and 13 mol% $YbO_{1.5}$, comparable to the work of Gonzalez et al. [26]. The ternary compositions analyzed outwith join $Yb_{(0.15+0.6x)}Nb_{0.25x}Zr_{(0.85-0.85x)}O_{(1.93-0.18x)}$ $(0 \leqslant x \leqslant 1)$ in the direction of increasing niobia, were all shown to be poly phasic. The low ytterbia, high zirconia limit of the cubic defect fluorite solid solution in the system $YbO_{1.5}$–$NbO_{2.5}$–ZrO_2 is, therefore, shown to very similar to that found in the closely related yttria-doped system, Figs. 1 and 2.

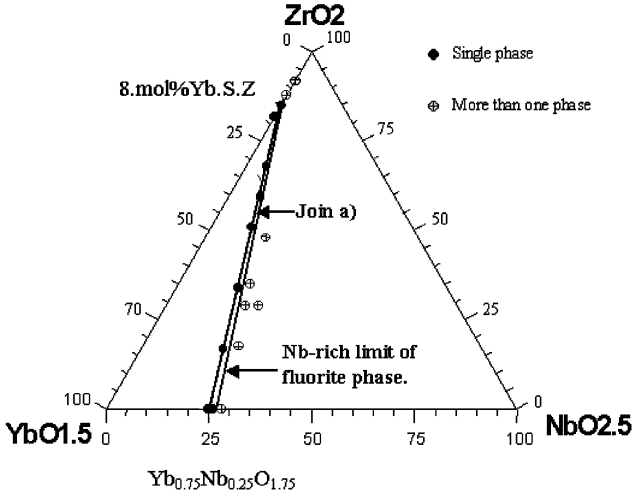

Fig. 2. The Nb-rich limit of the cubic defect fluorite solid solution in the system $YbO_{1.5}$–$NbO_{2.5}$–ZrO_2. Compositions analyzed are indicated. Join (a) = $Yb_{(0.15+0.6x)}Nb_{0.25x}Zr_{(0.85-0.85x)}O_{(1.93-0.18x)}$ $(0 \leqslant x \leqslant 1)$, N_B. This join links composition $Y_{0.15}Zr_{0.85}O_{1.93}$ and $Y_{0.75}Nb_{0.25}O_{1.75}$.

Lattice parameters of compositions on the joins $R_{(0.15+0.6x)}Nb_{0.25x}Zr_{(0.85-0.85x)}O_{(1.93-0.18x)}$, R = Y or Yb $(0 \leqslant x \leqslant 1)$, are plotted in Fig. 3 as a function of composition. As expected from ionic radii considerations, Yb containing compositions have smaller unit cells than their Y containing counterparts.

3.2.2. *Ionic conductivity of join* $Yb_{(0.15+0.6x)}Nb_{0.25x}Zr_{(0.85-0.85x)}O_{(1.93-0.18x)}$ $(0 \leqslant x \geqslant 1)$

Fig. 4 shows the temperature dependence of ionic conductivity for joins $R_{(0.15+0.6x)}Nb_{0.25x}Zr_{(0.85-0.85x)}O_{(1.93-0.18x)}$, R = Y or Yb, where $x = 0$, 0.3, 0.6, 0.8 and 1.0. This join links the compositions $R_{0.15}Zr_{0.85}O_{1.93}$ (8 mol% R_2O_3–ZrO_2) and $R_{0.75}Nb_{0.25}O_{1.75}$. Two observations can be drawn from these results: Firstly, the conductivity behavior of Y and Yb-doped samples are very similar, in concord with results on the binary R_2O_3–ZrO_2 join by Strickler and Carlson [24] for these dopants. Secondly, the level of ionic conductivity is slightly enhanced in those compositions that contain the larger dopant, although it must be noted that the magnitude of this enhancement is small and close to expected experimental error. However, the enhancement is observed to be uniform throughout the join and is also in agreement with the trend reported for the comparable fluorite composition $R_{0.8}Ta_{0.2}O_{1.7}$, where R = Gd, Y, Er, Yb by Yoshimura et al. [27].

Plotting low-temperature (<650°C) activation energy and conductivity pre-factors for the join $R_{(0.15+0.6x)}Nb_{0.25x}Zr_{(0.85-0.85x)}O_{(1.93-0.18x)}$, where R = Y and Yb, as a function of R content illustrates some interesting features, Fig. 5 (note that low-temperature

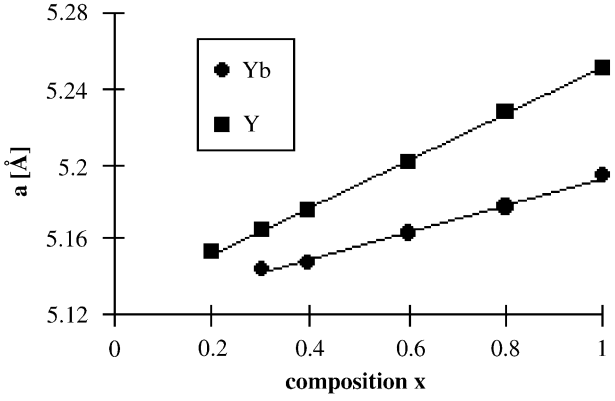

Fig. 3. Lattice parameters vs composition along join $R_{(0.15+0.6x)}Nb_{0.25x}Zr_{(0.85-0.85x)}O_{(1.93-0.18x)}$, R = Yb or Y $(0 \leqslant x \leqslant 1)$, N_B. This join links composition $R_{0.15}Zr_{0.85}O_{1.93}$ and $R_{0.75}Nb_{0.25}O_{1.75}$.

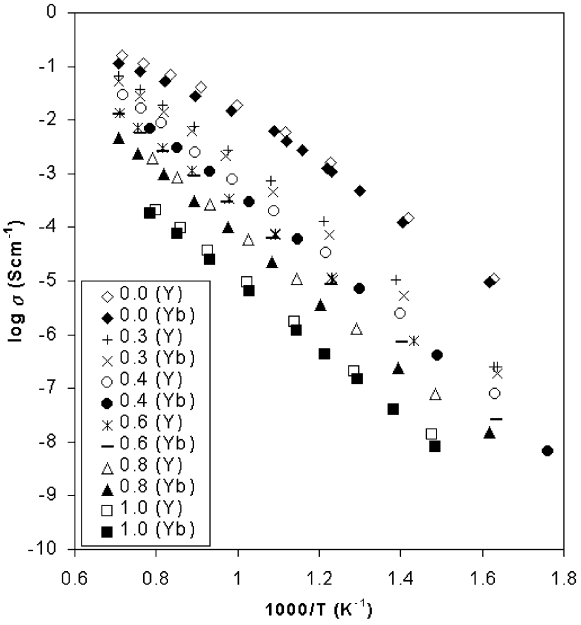

Fig. 4. The temperature dependence of bulk ionic conductivity for join $R_{(0.15+0.6x)}Nb_{0.25x}Zr_{(0.85-0.85x)}O_{(1.93-0.18x)}$, R = Yb or Y ($0 \leqslant x \leqslant 1$), N_B. This join links composition $R_{0.15}Zr_{0.85}O_{1.93}$ and $R_{0.75}Nb_{0.25}O_{1.75}$.

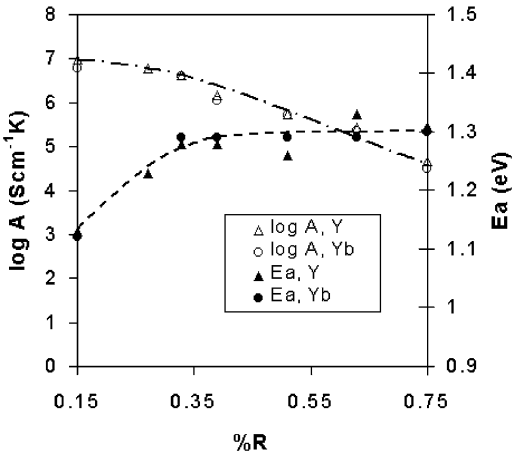

Fig. 5. The low-temperature (<650°C) activation energies and conductivity pre-factors for bulk ionic conductivity along the join $R_{(0.15+0.6x)}Nb_{0.25x}Zr_{(0.85-0.85x)}O_{(1.93-0.18x)}$, R = Yb or Y ($0 \leqslant x \leqslant 1$), as a function of R-content N_B. This join links composition $R_{0.15}Zr_{0.85}O_{1.93}$ and $R_{0.75}Nb_{0.25}O_{1.75}$.

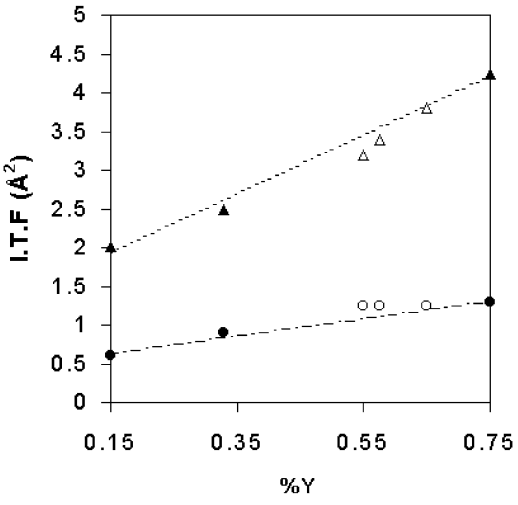

Fig. 6. Metal (circles) and oxygen (triangles) static isotropic temperature factors (ITF) as a function of Y-content for compositions on both joins (a) = $Y_{(0.15+0.6x)}Nb_{0.25x}Zr_{(0.85-0.85x)}O_{(1.93-0.18x)}$, (closed symbols) and (b) = $Y_{(0.5+0.25x)}Nb_{0.25x}Zr_{(0.5-0.5x)}O_{1.75}$ (open symbols) ($0 \leqslant x \leqslant 1$) shown in Fig. 1. Data for join (b) is from Ref. [10].

data is analyzed because elevated temperature leads to curvature of Arrhenius plots in compositions containing low R concentrations, due to breakup of ordered microdomains [9,10,12]). The conductivity behavior of Y and Yb containing compositions are almost identical. Activation energy rapidly increases with R content until 20–30%R above which activation energy tends to a constant around 1.3 eV. Conductivity pre-factor shows the inverse behavior decreasing with increasing R content. When activation energy is effectively constant, at high R contents, a linear decrease in conductivity pre-factor with R content is observed.

Due to the similarity of the conductivity behavior of the Y and Yb containing systems an explanation is offered based on structural data for $YO_{1.5}$–$NbO_{2.5}$–ZrO_2 [10,11]. Fig. 6 re-plots static isotropic temperature factors (ITF) obtained by neutron diffraction for the join $Y_{(0.5+0.25x)}Nb_{0.25x}Zr_{(0.5-0.5x)}O_{1.75}$, $0 \leqslant x \leqslant 1$, of constant vacancy concentration [10] together with new data along the join $Y_{(0.15+0.6x)}Nb_{0.25x}Zr_{(0.85-0.85x)}O_{(1.93-0.18x)}$ as a function of Y-content. The magnitude of the static factor reflects the mean local displacement of the ions from the ideal fluorite lattice positions, a phenomenon suggested to be due to local ordering [10,29]. Fig. 6 shows that the displacement of the ions from their ideal positions is quite clearly dominated by the Y-content. As Y-content increases both metal and oxygen ITFs increase, suggesting that local ordering has occurred on both cation and anion lattices in order to accommodate this large ion. Parallels can be drawn with the conductivity results, such as the occurrence of a decrease in pre-exponential factor for conductivity and, in the case of low defect concentrations, an increase in activation energy as the average position of the ions becomes shifted further from their ideal sites. One can envisage that the extent of microdomains with ions shifted from their ideal positions increases with increasing R-content, as a result of local ordering on the anion lattice. In these heavily substituted compositions, therefore, the anion ordering cannot be easily broken up by increases in temperature. For this reason a change in activation energy for conduction with temperature is only observed in compositions containing small concentrations of Y or Yb, in which both cations and

anions are sited close to their theoretical fluorite positions.

In summary, the ionic conductivity behavior of Yb and Y-substituted systems are very similar, a reflection of the close physical and chemical properties of these elements. Although, small decreases in activation energy for increases in Nb concentration have been observed in previous work [9,10] the conductivity behavior of the systems $YO_{1.5}$–$NbO_{2.5}$–ZrO_2 and $YbO_{1.5}$–$NbO_{2.5}$–ZrO_2 are clearly shown to be dominated by the Y or Yb-content, decreasing as the local order on the anion and cation lattices increases.

3.3. System CaO–$NbO_{2.5}$–ZrO_2

In both the yttrium and ytterbium ternary systems, compositions which contain significant niobium concentrations, have been shown to offer quite low values of ionic conductivity. If one considers the use of Rare Earth dopants greater in size than Y such as La, Nd or Gd, these elements have been shown to not stabilize the cubic phase on the binary join R_2O_3–Nb_2O_5 (where R = Rare Earth) [27]. Therefore, these larger dopant ions are not thought to offer such extensive cubic defect fluorite solid solutions as in the case of yttrium or ytterbium. Interest, therefore, turned to other types of stabilizing dopant such as CaO.

Ca is of large ionic radius (1.12 Å from Shannon [28]). It is also divalent, one dopant cation of Ca produces one vacancy compared to only $\frac{1}{2}$ a vacancy for a Y-dopant ion. For this reason one would perhaps expect the defect fluorite phase to be stabilized with a lower overall concentration of dopants than in the trivalent dopant-based systems. This hypothesis is confirmed in binary systems with zirconia. Only 11.5 mol% CaO is needed to stabilize the cubic phase compared with 14.5 mol% in the case of $YO_{1.5}$ [11]. In the ternary CaO–$NbO_{2.5}$–ZrO_2 system, compositions of the fluorite phase may be found with a high niobium content, which contain less stabilizing dopant than that obtainable in the Y or Yb-stabilized systems. This lower concentration of stabilizing dopant may affect the level of ionic conductivity observed.

Strickler and Carlson [24] investigated the isothermal conductivity behavior of both the Y_2O_3–ZrO_2 and the CaO–ZrO_2 systems with composition near the limit of the dilute range [25]. The maximum in the conductivity vs dopant composition plots, was shown to be higher for Y_2O_3-doped zirconia than CaO-doped zirconia (10^{-1} S cm^{-1} for Y_2O_3–ZrO_2 cf. 5×10^{-2} S cm^{-1} for CaO–ZrO_2 at 1000°C), whilst the concentration of stabilizing dopant at the position of the maxima were shown to be similar for the two systems (14.8 mol% $YO_{1.5}$ cf. 13 mol% CaO).

There is a shortage of data for these systems at very high vacancy concentrations, but the work by Strickler and Carlson plots conductivity data for the two systems Zr(Ca or Y)O_{2-y}, up to deviations from stoichiometry equal to $y=0.2$ [24]. In the concentrated range, the calcia-doped compositions show a higher isothermal conductivity for a specific vacancy concentration, than the yttrium-doped compositions. An example of this is given if one compares the conductivity of 13 mol% CaO, with a composition in the system Y_2O_3–ZrO_2 with a comparable vacancy concentration (i.e. 26 mol% $YO_{1.5}$). It is observed that the CaO-doped species has the highest conductivity (5×10^{-2} S cm^{-1} for CaO–ZrO_2 cf. $\sim10^{-2}$ S cm^{-1} for Y_2O_3–ZrO_2 at 1000°C).

This section investigates the calcia-doped system CaO–$NbO_{2.5}$–ZrO_2. The extent of the defect fluorite range is determined and the conductivity of compositions which offer the smallest concentration of stabilizing dopant for a fixed niobium content are compared to similar compositions in the yttria-doped system.

3.3.1. Extent of the cubic defect fluorite phase

Work on the three binary joins CaO–ZrO_2, CaO–Nb_2O_5, and ZrO_2–Nb_2O_5 has been published by the following authors, Stubican et al. [30], Ibrahim et al. [31], and Roth et al. [32], respectively. Important phases to consider, are those of the defect fluorite solid solution on the join CaO–ZrO_2, between the compositions ~11–20 mol% CaO and that of the composition $Ca_2Nb_2O_7$ on the join CaO–Nb_2O_5.

The composition $Ca_2Nb_2O_7$ shows many allotropes. Low-temperature hydrothermal synthesis has been shown by Jacobson et al. [33] to yield a typical (II, V) pyrochlore phase, which is stable on heating to ca. 650°C. Between the temperatures of 650°C and 700°C, this low-temperature phase transforms slowly to a perovskite-based structure. Two perovskite-based allotropes have been investigated. A monoclinic variety studied by Brandon and Megaw [34] and an orthorhombic type studied comprehensively by Carpy et al. [35].

Whilst the structure of the pyrochlore allotrope can be very simply related to that of the fluorite phase, the same cannot be easily stated for the structures of the perovskite-based allotropes and that of the fluorite cell. The structure of the perovskite allotropes are most easily described as being derived from an ideal perovskite structure consisting of slabs of distorted corner-sharing NbO_6 octahedra and Ca atoms. The slabs are shifted relative to one another by heights of one-half the basic perovskite unit edge to form the documented $Ca_2Nb_2O_7$ structure. If one must describe the perovskite-related structure of $Ca_2Nb_2O_7$ as being derived from that of fluorite it is possible, but is rather complex. It involves the loss of an $\frac{1}{8}$ of the anions, to producing edge-sharing NbO_6 octahedra (similar to that observed in the C-type Y_2O_3 structure). These edge-sharing octahedra then must become corner sharing to

form slabs of perovskite-type NbO_6 octahedra which are then displaced.

A compositional join drawn between a composition on the defect fluorite solid solution shown on the binary $CaO–ZrO_2$ join, which links with the composition $Ca_2Nb_2O_7$ on the $CaO–Nb_2O_5$ join, should, at this temperature, be hoped to possess compositions that would convert from that of the defect fluorite structure, to that of a mixture of the fluorite and perovskite-based structures as the join is descended. It is hoped that the defect fluorite phase might extend away from the binary $CaO–ZrO_2$ join into the ternary system, to produce compositions of the defect fluorite structure which contain niobium, before this complex transformation to the perovskite-based structure occurs.

Many compositions were, therefore, made on a join linking the defect fluorite composition $Zr_{0.85}Ca_{0.15}O_{1.85}$ and the perovskite-based composition $Ca_2Nb_2O_7$. The compositions analyzed and the limits of the cubic defect fluorite phase at the two sintering temperatures 1400°C and 1500°C are presented in Fig. 7. Samples outside the cubic defect fluorite region showed the presence of additional phases, Table 1. The most common additional phases were those of $CaZrO_3$ and the monoclinic phase of zirconia. Compositions that show the additional phase denoted * in Table 1, lie on the join between $Zr_{0.85}Ca_{0.15}O_{1.85}$ and $Ca_2Nb_2O_7$. The additional phase is, therefore, possibly of the orthorhombic distorted perovskite end composition $Ca_2Nb_2O_7$. Reflections that were observable fitted with this suggestion. In all these compositions, additional binary phases such as $CaZr_4O_9$, $CaNb_2O_6$, and $Nb_2Zr_6O_{17}$ were shown to be absent.

At 1400°C the cubic defect fluorite solid solution is shown to exist between compositions ~12–20 mol% CaO on the binary join $CaO–ZrO_2$ and stretch just beyond the composition $Ca_{0.2375}Zr_{0.6375}Nb_{0.125}O_{1.825}$ containing 12.5 mol% Nb on the join between $Ca_{0.15}Zr_{0.85}O_{1.85}$ and $Ca_2Nb_2O_7$. The width of the solid solution lying on the binary join fits very well with the work by Stubican and Ray [30]. At the higher temperature of 1500°C the width of the defect fluorite solid solution on the binary join to remains effectively constant, but to now stretches to encompass the composition $Ca_{0.255}Zr_{0.595}Nb_{0.15}O_{1.82}$, which contains 15 mol% Nb.

The size of the defect fluorite solid solution in the system $CaO–Nb_2O_5–ZrO_2$ is therefore seen to be small, but to increase with increasing temperature. The maximum concentration of niobium that can exist in the cubic phase at temperatures less than or equal to 1500°C is 15 at%.

The composition $Ca_{0.255}Zr_{0.595}Nb_{0.15}O_{1.82}$ was annealed at 1000°C for 8 days. No change to the X-ray diffraction pattern obtained for the sample was observed. This suggests that phases which exist at higher temperatures can be quenched in.

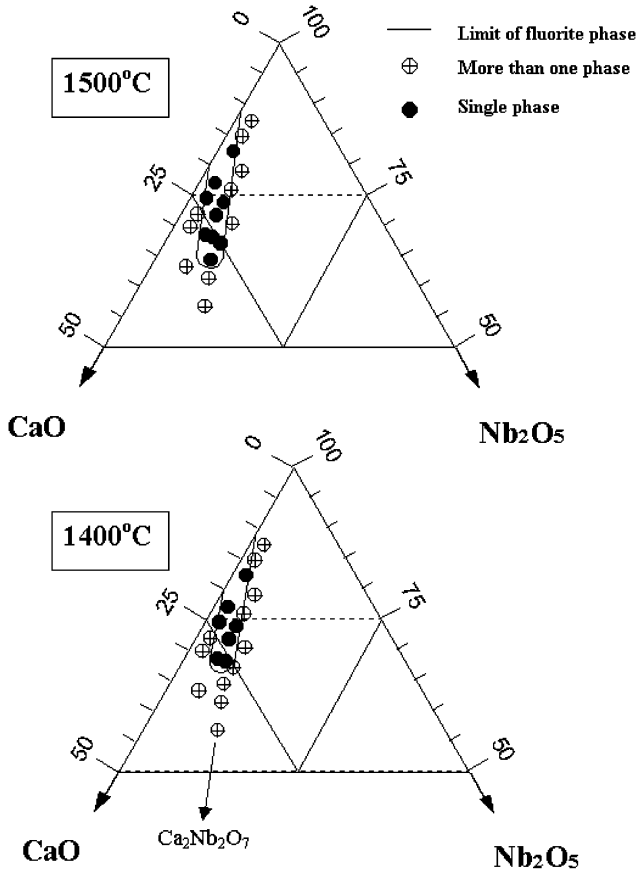

Fig. 7. The limit of the defect fluorite solid solution in the system $CaO–Nb_2O_5–ZrO_2$ quenched from 1400°C to 1500°C. The compositions analyzed are shown.

3.3.2. *Ionic conductivity of $Ca_{0.255}Zr_{0.595}Nb_{0.15}O_{1.82}$*

In the previous section the composition $Ca_{0.255}Zr_{0.595}Nb_{0.15}O_{1.82}$ was shown to contain the highest niobium content (15 mol% Nb), obtainable for a cubic defect fluorite phase, at the maximum sintering temperature of 1500°C. It also contains the lowest calcium/zirconium ratio for this niobium content. From the results on the $YO_{1.5}–NbO_{2.5}–ZrO_2$ system [7,8], this level of niobium was shown to be the minimum concentration necessary in order to exhibit a significant electronic contribution to the level of total conductivity in reducing conditions. The composition $Ca_{0.255}Zr_{0.595}Nb_{0.15}O_{1.82}$ is, therefore, believed to offer the best properties of combined ionic and electronic conduction available in the Ca stabilized system at sintering temperatures of 1500°C and below.

Fig. 8 compares the bulk ionic conductivity of the composition $Ca_{0.255}Zr_{0.595}Nb_{0.15}O_{1.82}$ with the composition $Y_{0.51}Zr_{0.34}Nb_{0.15}O_{1.82}$. The composition $Y_{0.51}Zr_{0.34}Nb_{0.15}O_{1.82}$ was shown to offer the highest level of ionic conductivity for a niobium content of 15 mol%, obtainable in the yttrium stabilized system [7,8]. These two compositions are directly comparable as they have the

Table 1
The phases present in room temperature X-ray patterns of compositions from the system $CaO–Nb_2O_5–ZrO_2$, quenched from the two sintering temperatures 1400°C and 1500°C

Composition	Phases in room temperature X-ray patterns from 1400°C			Phases in room temperature X-ray patterns from 1500°C		
	$CaZrO_3$	c-ZrO_2	m-ZrO_2	$CaZrO_3$	c-ZrO_2	m-ZrO_2
$Ca_{0.15}Zr_{0.8}Nb_{0.05}O_{1.875}$		s			s	
$Ca_{0.2}Zr_{0.75}Nb_{0.05}O_{1.825}$		s			s	
$Ca_{0.25}Zr_{0.7}Nb_{0.05}O_{1.775}$	s	s		s	s	
$Ca_{0.1}Zr_{0.85}Nb_{0.05}O_{1.925}$		s	s		s	s
$Ca_{0.125}Zr_{1.825}Nb_{0.05}O_{1.90}$		s	m		s	m
$Ca_{0.225}Zr_{0.725}Nb_{0.05}O_{1.8}$		s			s	
$Ca_{0.3}Zr_{0.6}Nb_{0.1}O_{1.75}$	m	s		m	s	
$Ca_{0.2375}Zr_{0.6375}Nb_{0.125}O_{1.825}$		s			s	
$Ca_{0.23}Zr_{0.62}Nb_{0.15}O_{1.845}$		s	m		s	
$Ca_{0.18}Zr_{0.72}Nb_{0.1}O_{1.87}$		s	m		s	w
$Ca_{0.15}Zr_{0.75}Nb_{0.1}O_{1.9}$		s	s		s	s
$Ca_{0.25}Zr_{0.65}Nb_{0.1}O_{1.8}$		s			s	
$^{*}Ca_{0.269}Zr_{0.561}Nb_{0.17}O_{1.816}$		s	w		s	
$^{*}Ca_{0.29}Zr_{0.51}Nb_{0.2}O_{1.81}$		s	w		s	
$Ca_{0.255}Zr_{0.595}Nb_{0.15}O_{1.82}$	w	s			s	
$Ca_{0.2}Zr_{0.7}Nb_{0.1}O_{1.85}$		s			s	
$Ca_{0.22}Zr_{0.68}Nb_{0.1}O_{1.83}$		s			s	
$Ca_{0.20}Zr_{0.65}Nb_{0.15}O_{1.875}$		s	m		s	m
$Ca_{0.27}Zr_{0.68}Nb_{0.05}O_{1.175}$	s	s		s	s	

s = strong, m = medium, w = weak and refer to the relative intensities of the phases observable by X-ray diffraction. The label * refers to the presence of small traces of an additional phase in these samples, where the intensity of the lines of this additional phase were too low and too few to be accurately identified.

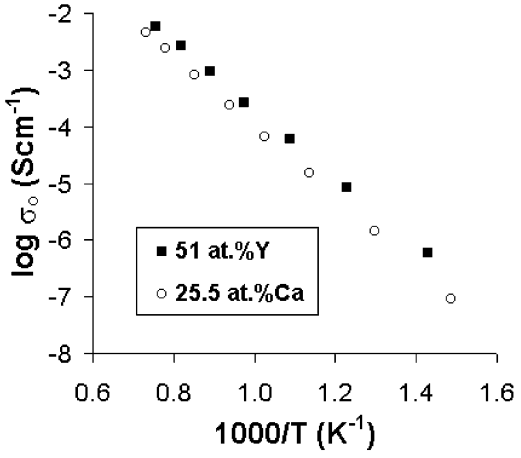

Fig. 8. The temperature dependence of bulk ionic conductivity of $Ca_{0.255}Zr_{0.595}Nb_{0.15}O_{1.82}$ and $Y_{0.51}Zr_{0.34}Nb_{0.15}O_{1.82}$. These compositions represent the minimum Ca or Y contents required to stabilize the cubic defect fluorite phase in compositions containing 15% Nb at 1500°C.

same niobium content and contain the same vacancy concentration. Table 2 gives the lattice parameter the activation energy and the pre-exponential factor for conduction for each composition. The conductivity for the two compositions is observed to be similar and to converge at higher temperatures giving a level of ionic conductivity at 1000°C of approximately $2.5 \times 10^{-3}\,S\,cm^{-1}$ for each composition. Table 2 shows the activation energies for both compositions to be high in magnitude. The CaO-doped composition is observed to have a slightly higher activation energy and pre-exponential factor for conduction.

The conclusion to be drawn from these results is that, despite the lower Ca concentration than that of Y and the lower lattice parameter of the Ca-containing composition, the conduction behavior in these two compositions is similar. Due to the nature of the phase diagrams in both the Ca-stabilized and Y-stabilized cases, the level of 15 mol% niobium can only exist in compositions where the concentration of other defects are high. At these high dopant concentrations the observed conduction behavior may have entered a plateau-type region in the level of conductivity obtainable, similar to that observed for the system $YO_{1.5}–NbO_{2.5}–ZrO_2$ [7–12], where high activation energies around 1.3 eV are typical. This emanates from the formation of microdomains of existing ordered phases, which hinder vacancy movement [10,11]. Whilst electron diffraction studies have showed that these ordered microdomains in the $YO_{1.5}–NbO_{2.5}–ZrO_2$ system can be considered to be a mixture of C-type and distorted pyrochlore (P-type structure) [11], possible ordered phases can also be suggested for the Ca-containing system. The presence of microdomains of the orthorhombic phase $CaZr_4O_9$ has been suggested by Allpress and Rossell to exist in the system $Zr(Ca)O_{2-y}$ [36], whilst the presence of small microdomains of the phase

Table 2
Regression parameters of the Arrhenius model for bulk ionic conductivities in air

Composition	Activation energy (eV)	Pre-exponential factor (10^5) ($S\,cm^{-1}\,K$)	Lattice parameter (Å) ± 0.0005
$Ca_{0.255}Zr_{0.595}Nb_{0.15}O_{1.82}$	1.31	4.2	5.1453
$Y_{0.51}Zr_{0.34}Nb_{0.15}O_{1.82}$	1.26	3.6	5.2013

$Ca_2Nb_2O_7$ may also occur in the ternary system $Zr(Ca)(Nb)O_{2-y}$. Interestingly, all the phases mentioned contain MO_6 octahedra (where M is a cation), typical of a Bevan-type local arrangement of vacancies [36]. For these two compositions, the compositional vacancy concentration is equal. Therefore, if one imagines all vacancies to be involved in Bevan-type aggregates involving vacancy pairs, the number of aggregate species in both compositions must also be equal. This observation perhaps offers further explanation of the similarity of conduction behavior between the two compositions.

For compositions containing 15 mol% Nb no significant improvement in isothermal conductivity at 1000°C can be obtained over the yttrium-stabilized system by the use of calcium as the stabilizing dopant.

3.4. The transition element dopant

The highest level of ionic conductivity for a specific niobium concentration, in the system Y_2O_3–Nb_2O_5–ZrO_2, was exhibited along the low yttria/high zirconia edge of the solid solution given by the equation $(1-x)Y_{0.15}Zr_{0.85}O_{1.93-x}Y_{0.75}Nb_{0.25}O_{1.75}$. The conduction properties of three compositions from this join were compared to their titania-doped equivalents. All compositions showed X-ray diffraction patterns characteristic of the defect fluorite structure. Lattice parameters are shown in Table 3. Titanium in the 4+ oxidation state has a very similar ionic radius to that of niobium in the 5+ oxidation state. Nevertheless, lattice parameters of the niobia-doped samples are larger than their titania-doped counterparts, in accord with their lower vacancy concentration.

The isothermal conductivities at various temperatures are plotted in Fig. 9, against yttrium content. At small dopant concentrations, the level of ionic conductivity is shown to be improved with niobium doping over that which is obtainable in samples of the same cation stoichiometry doped with titanium. This can be associated with the vacancy concentration. An increase in ionic conduction with decreasing vacancy concentration is characteristic of zirconia-based fluorite compositions when defect concentration is low [25]. However, in the heavily substituted samples $Y_{0.39}Zr_{0.51}Ti_{0.1}O_{1.805}$, $Y_{0.51}Zr_{0.34}Ti_{0.15}O_{1.745}$ and $Y_{0.51}Zr_{0.34}Nb_{0.15}O_{1.82}$ the isothermal conductivities are shown to be almost

Table 3
Regression parameters of the Arrhenius model for bulk ionic conductivities in air

Composition	Activation energy (eV)	Pre-exponential factor ($\times 10^5$) ($S\,cm^{-1}\,K$)	Lattice parameter (Å) ± 0.0005
$Y_{0.27}Zr_{0.68}Nb_{0.05}O_{1.89}$	l.t. = 1.23 h.t. = 1.01	l.t. = 60.3 h.t. = 3.2	5.1533
$Y_{0.39}Zr_{0.51}Nb_{0.1}O_{1.85}$	1.28	14.8	5.1760
$Y_{0.51}Zr_{0.34}Nb_{0.15}O_{1.82}$	1.26	3.6	5.2013
$Y_{0.27}Zr_{0.68}Ti_{0.05}O_{1.865}$	1.30	16.6	5.1524
$Y_{0.39}Zr_{0.51}Ti_{0.1}O_{1.805}$	1.36	12.9	5.1578
$Y_{0.51}Zr_{0.34}Ti_{0.15}O_{1.745}$	1.31	7.6	5.1690
$Y_{0.25}Zr_{0.60}Ti_{0.15}O_{1.875}$	1.17	6.2	5.1213

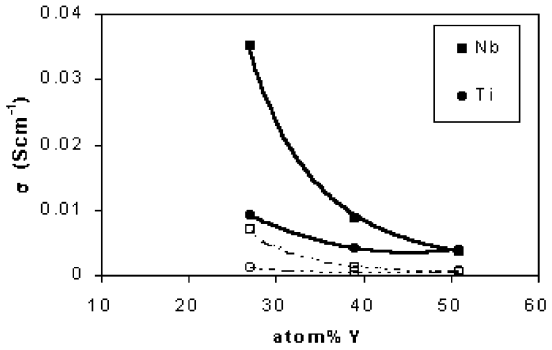

Fig. 9. Bulk isothermal conductivities as a function of Y-content for the Ti and Nb-containing compositions listed in Table 3, at 1000°C and 800°C.

constant allowing comparison to be drawn with Fig. 5, which showed convergence in conductivity behavior for samples containing high defect concentrations.

3.5. The systems $YO_{1.5}$–TiO_2–ZrO_2, CaO–TiO_2–ZrO_2 and $GdO_{1.5}$–TiO_2–ZrO_2

3.5.1. Extent of the cubic defect fluorite phase

Detailed experimental phase diagrams of the system $YO_{1.5}$–TiO_2–ZrO_2 [17,18] exist, which support the theoretically calculated phase diagram published by Yokokawa et al. [22], and show extensive defect fluorite solid solution. The Gd-containing system $GdO_{1.5}$–TiO_2–ZrO_2 is also published [19] and interestingly exhibits two distinct regions of cubic defect fluorite phase, one located in the Gd-rich region of the phase diagram and another in the Zr-rich region. To date, most attention in has been concentrated in the pyrochlore and Gd-rich fluorite solid solutions [19], whilst the Zr-rich fluorite region remains poorly characterized. For the present study we are interested in these Zr-rich defect fluorite materials which contain minimum concentrations of the large aliovalent dopant, as it is these compositions which are expected to offer the highest

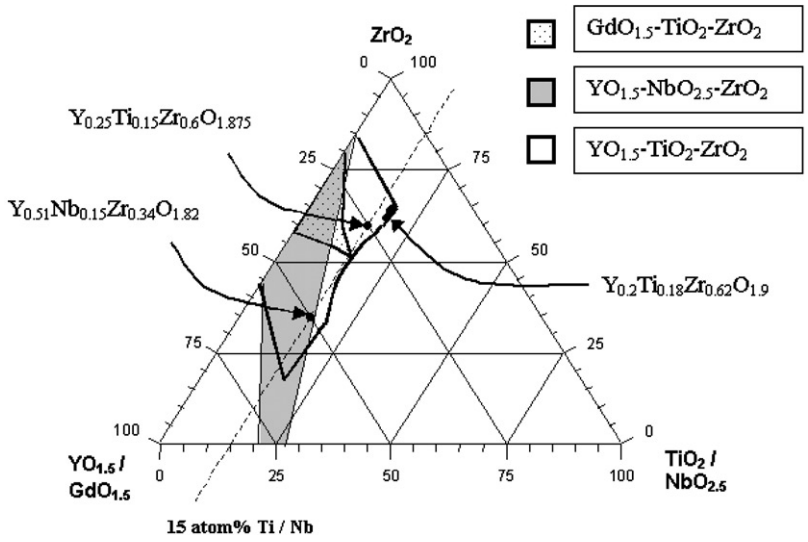

Fig. 10. The extent of the cubic defect fluorite solid solution in the systems $YO_{1.5}$–$NbO_{2.5}$–ZrO_2 [8], $YO_{1.5}$–TiO_2–ZrO_2 [17] and $GdO_{1.5}$–TiO_2–ZrO_2 [19] quenched from 1500°C. Only Zr-rich solid solutions are presented. The extent of the solid solution is much greater in the $YO_{1.5}$–TiO_2–ZrO_2 system in the direction of low Y.

ionic conductivities. The extent of the defect fluorite solid solution in this Zr-rich fluorite region [19] is reproduced in Fig. 10 overlaid with that of the $YO_{1.5}$–TiO_2–ZrO_2 system [17] and the niobium-containing system [8] $YO_{1.5}$–$NbO_{2.5}ZrO_2$ all at 1500°C. Solid state phase relationships of the system CaO–TiO_2–ZrO_2 have been previously reported [20,21]; however, it seems that the cubic defect fluorite solid solution is extremely limited, barely entering the ternary system. Slight increase in extent of the solid solution is observed with increasing temperature, but it is thought that even at 1500°C, the fluorite solid solution in this system will be very limited and, subsequently, is not included in Fig. 10.

Fig. 10 clearly demonstrates that the extent of the defect fluorite solid solution is much greater in the Y_2O_3–TiO_2–ZrO_2 system in the direction of low Y, than in any of the other systems examined, suggesting fluorite compositions containing up to 18 at% Ti can exist with only 15–20 at% Y required to stabilize the phase.

3.5.2. *Ionic conductivity of system $YO_{1.5}$–TiO_2–ZrO_2*

Much work has been done on the composition dependence of ionic conductivity in the defect fluorite solid solution of this system [1,2,4,10,18,23]. The reported trends unequivocally support the trends observed in niobium-containing $YO_{1.5}/YbO_{1.5}$–$NbO_{2.5}$–ZrO_2 systems. The conductivity behavior is again dominated by the concentration of the large rare earth dopant, decreasing dramatically as concentration increases [1,10,23], whilst, at a constant rare earth concentration, increases in transition element content lead to small decreases in both total conductivity and activation energy for conduction [1,10]. Fig. 11 demonstrates this relationship of activation energy on Y and Ti

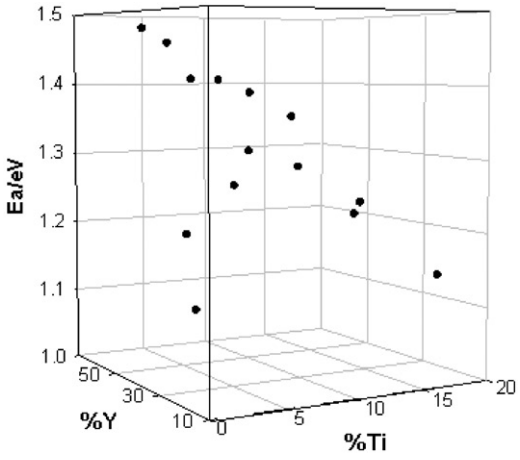

Fig. 11. The dependence of activation energy for bulk ionic conductivity on Y and Ti-content in the system $YO_{1.5}$–TiO_2–ZrO_2.

content. The reduction of activation energy with increasing Ti content is suggested to be related to the decrease in lattice parameter [10]. A similar statement to that of the niobium-containing systems can, therefore, be stated. For any fixed Ti-content the defect fluorite compositions of highest conductivity will be those on the low Y/high Zr edge of the solid solution.

Fig. 12 presents the temperature dependence of ionic conductivity for the compositions $Y_{0.25}Ti_{0.15}Zr_{0.6}O_{1.875}$, and $Y_{0.51}Nb_{0.15}Zr_{0.34}O_{1.82}$, indicated in Fig. 10. The ionic conductivity of the compositions is shown to decrease as Y-content increases, supporting the trend that ionic conductivity is dominated by the stabilizing Y concentration in these system types. The ionic conductivity of $Y_{0.25}Ti_{0.15}Zr_{0.6}O_{1.875}$, containing 15 at% Ti, is much greater than the optimum conducting composition containing 15 at% Nb obtainable in the Nb system,

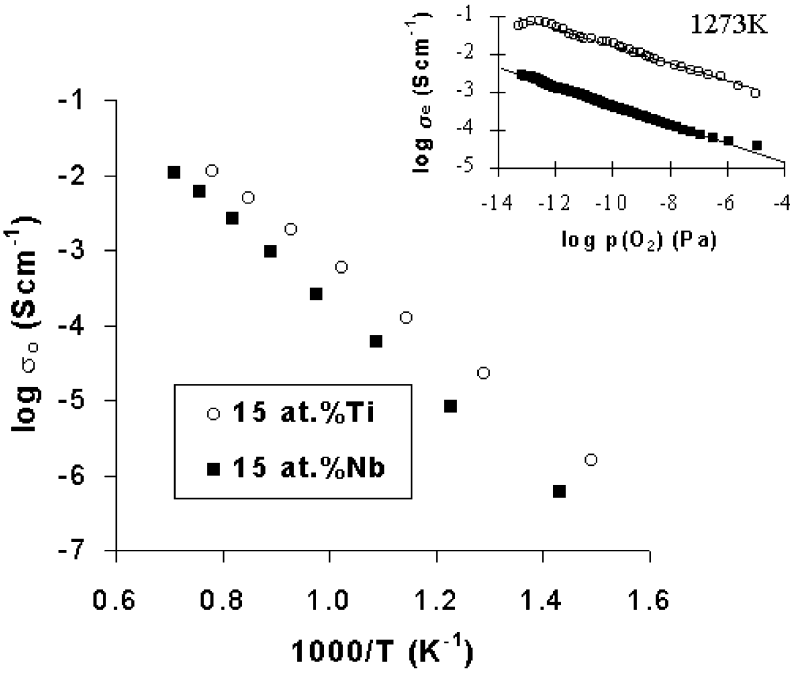

Fig. 12. The temperature dependence of bulk ionic conductivity $Y_{0.25}Ti_{0.15}Zr_{0.6}O_{1.875}$ and $Y_{0.51}Nb_{0.15}Zr_{0.34}O_{1.82}$. The Nb-containing composition represents the peak mixed conducing composition for a content of 15% transition element available in the system $YO_{1.5}$–$NbO_{2.5}$–ZrO_2. Inset shows the pO_2 dependence of electronic conductivity for the same compositions taken from Ref. [7].

$Y_{0.51}Nb_{0.15}Zr_{0.34}O_{1.82}$. The nature of these two fluorite solid solutions allows compositions containing 15 at% transition element to exist with less than half the Y-content required to stabilize the phase in the titanium system, compared to that required in the niobium system. This difference in composition dominates the level of ionic conductivity and therefore, subsequently also the total conductivity values obtained. The inset in Fig. 12 calculated from total conductivity vs pO_2 measurements for these compositions published in Ref. [7], also shows that the electronic contribution is greater for 15 at% Ti than 15 at% Nb, a factor resulting from more facile reduction of Ti than Nb in these compositions (reduction of 8.7% Ti^{4+} to Ti^{3+} cf. 3.6% Nb^{5+} to Nb^{4+} in 10% H_2/N_2 at 1000°C [7]).

Peak mixed conduction is offered by compositions containing 18 at% Ti at the Zr-rich limit of the defect fluorite solid solution in the system $YO_{1.5}$–TiO_2–ZrO_2, Fig. 10. Previous work reports that these peak 18 at% Ti compositions show slight increase in both ionic and electronic conductivities with decreasing Y-content [23].

4. Conclusions

The magnitude of ionic conductivity is dominated by the concentration of the rare earth dopant, a result suggested to be related to defect association and local ordering. For a fixed and low rare earth content, substitution of Zr by Ti or Nb causes slight decreases in ionic conductivity and activation energy. When both Zr and rare earth content are fixed, improvements in ionic conductivity can be induced by Nb doping over that of Ti doping due to a decreased vacancy concentration. At high defect concentrations conductivity is low and insensitive to such compositional change, in this range activation energies are observed constant and high, around 1.3 eV. A greater electronic enhancement to total conductivity in reducing conditions is offered by Ti-containing compositions with respect to Nb-containing compositions due to more facile reduction of Ti.

For any fixed concentration of transition element, the defect fluorite compositions of highest conductivity will be those on the low rare earth/high Zr edge of the solid solution. Due to the limited extent of solid solution in this direction, the best-mixed conducing compositions can only be offered in the system Y_2O_3–TiO_2–ZrO_2. The solid solution in the Y_2O_3–TiO_2–ZrO_2 system offers peak mixed conducing defect fluorite compositions containing up to 18 mol% Ti with less than 20% Y required to stabilize the cubic phase, which far exceed the mixed conductivities obtainable in all other systems here studied.

References

[1] A. Kaiser, A.J. Feighery, D.P. Fagg, J.T.S. Irvine, Ionics 4 (1998) 215.
[2] W.L. Worrell, Y. Uchimoto, P. Han, Electrochem. Soc. 97–24 (1998) 329.

[3] J.H. Kim, G.M. Choi, Solid State Ionics 130 (2000) 157.
[4] T. Lindergaard, C. Clausen, M. Mogensen, in: F.W. Poulsen, J.J. Bentzen, T. Jacobson, E. Skou, M.J.L. Ostergaard (Eds.), Proceedings of the 14th Riso International Symposium on Material Science, Roskilde, Denmark, 1993, p. 117.
[5] T. Ishihara, K. Sato, Y. Mizuhara, Y. Takita, Solid State Ionics 50 (1992) 227.
[6] N.A. Bondar, L.N.K. Oroleva, N.A. Toropov, Neorg. Mater. 5 (10) (1969) 1730.
[7] D.P. Fagg, J.T.S. Irvine, Ionics 4 (1998) 61.
[8] J.T.S. Irvine, D.P. Fagg, J. Labrincha, F.M.B. Marques, Catalysis Today 38 (1997) 467.
[9] J.T.S. Irvine, I.R. Gibson, D.P. Fagg, Ionics 1 (1995) 279.
[10] J.T.S. Irvine, A.J. Feighery, D.P. Fagg, S. García-Martín, Solid State Ionics 136 (2000) 879.
[11] S. García-Martín, M.A. Alario-Franco, D.P. Fagg, A.J. Feighery, J.T.S. Irvine, Chem. Mater. 12 (2000) 1729.
[12] D.P. Fagg, Ph.D. Thesis, University of Aberdeen, Scotland, 1996.
[13] J.-H. Lee, M. Yoshimura, Solid State Ionics 124 (1999) 185.
[14] J.-H. Lee, M. Yoshimura, Solid State Ionics 139 (3–4) (2001) 197.
[15] R. Wallenberg, R.L. Whithers, D.M. Bevan, J.G. Thompson, P. Barlow, B.G. Hyde, J. Less Common Met. 156 (1989) 1.
[16] R.L. Withers, J.G. Thompson, P.J. Barlow, J. Solid State Chem. 94 (1991) 89.
[17] A.J. Feighery, J.T.S. Irvine, D.P. Fagg, A. Kaiser, J. Solid State Chem. 143 (1999) 273.
[18] M.T. Colomer, P. Durán, A. Caballero, J.R. Jurado, Mater. Sci. Eng. A 229 (1997) 114.
[19] A.J. Feighery, J.T.S. Irvine, C. Zheng, J. Solid State Chem. 160 (2001) 302.
[20] D. Swenson, T.-G. Nieh, J.H. Fournelle, J. Am. Ceram. Soc. 81 (12) (1998) 3249.
[21] M.O. Figueiredo, A. Correia dos Santos, in: S. Meriani, C. Palmonari (Eds.), Zirconia 88: Advances in Zirconia Science and Technology, Elsevier Science, Essex, UK, 1989, p. 81.
[22] H. Yokokawa, T. Horita, N. Sakai, M. Dokiya, J. Van Herle, S.G. Kim, Denki Kagaku 64 (6) (1996) 690.
[23] S. Tao, J.T.S. Irvine, J. Solid State Chem. 165 (12–18) (2002) 12.
[24] D.W. Strickler, W.G. Carlson, J. Am. Ceram. Soc. 48 (6) (1965) 286.
[25] J.A. Kilner, B.C.H. Steele, in: O. Toft Sørensen (Ed.), Non-Stoichiometric Oxides, Academic Press Inc, New York, 1981, p. 233.
[26] M. González, C. Moure, J.R. Jurado, P. Durán, J. Mater. Sci. 28 (1993) 3451.
[27] S. Kim, M. Yashimira, M. Kakihana, M. Yoshimura, J. Alloys Compd. 192 (1993) 72.
[28] R.D. Shannon, Acta Crystallogr. A 32 (1976) 751.
[29] D.N. Argyriou, J. Appl. Crystallogr. 27 (1994) 155.
[30] V.S. Stubican, S.P. Ray, J. Am. Ceram. Soc. 60 (11) (1977) 534.
[31] M. Ibrahim, N. Bright, J. Rowland, J. Am. Ceram. Soc. 45 (7) (1962) 329.
[32] R. Roth, J. Waring, W. Brower, H. Parker, NBS Spec. Publ. 364 (1972) 183.
[33] J.T. Lewandowski, A.J. Jacobson, I.J. Pickering, Mater. Res. Bull. 27 (1992) 981.
[34] J.K. Brandon, H.D. Magaw, Philos. Mag. 21 (1970) 189.
[35] R. Potier, A. Carpy, M. Fayard, J. Galy, Phys. Stat. Sol. 30 (9) (1975) 683.
[36] H.J. Rossell, in: A.H. Hever, L.W. Hobbs (Eds.), Science and Technology of Zirconia, Advances in Ceramics, Vol. 3, American Ceramic Society, Columbus, OH, 1981, pp. 47–63.